

Development of Mathematical Model for Vibration Accelerated Wound Healing

Needs D¹, Blotter J¹, Dallon JC², Feland JB³

¹Department of Mechanical Engineering, Brigham Young University - Provo

²Department of Mathematics, Brigham Young University - Provo

³Department of Exercise Science, Brigham Young University - Provo

*Corresponding author: Blotter J, Department of Mechanical Engineering, Brigham Young University- Provo, UT 84602, Tel:+1-801-422-7820, Email: jblotter@byu.edu

Citation: Needs D, Blotter J, Dallon, JC, Feland JB (2022) Development of Mathematical Model for Vibration Accelerated Wound Healing. J Biostat Biometric App 7(1): 101

Abstract

Chronic wounds substantially reduce the quality of life for millions of people worldwide. As a result, researchers have developed various treatments and therapies to reduce the time for a wound to heal. Mathematical models that help better understand and predict the wound healing process have also been developed. This paper presents and validates a mathematical model known as the vibration enhanced wound healing model (VEWH) that includes the effects of vibration treatment in the wound healing process. The model is based on existing models of cutaneous wound healing but includes the effects of vibration on blood flow, macrophages, chemoattractant, and fibroblasts. These parameters were derived from published data on vibration accelerated wound healing of healthy mice. The VEWH model is confirmed with published experimental animal data that show vibration can reduce the wound healing time by 8%. The model reveals that vibration primarily affects healing through the mechanotransduction of vibration by fibroblasts into greater production of extracellular matrix. Model simulations agree with the validation data, with optimal healing predicted to occur with frequencies between 5 Hz and 25 Hz.

Keywords: Wound Healing, Vibration, Mathematical Model

List of abbreviations:

VEWH	Vibration enhanced wound healing
VEGF	Vascular endothelial growth factor
TGF- β	Transforming growth factor β
ECM	Extracellular matrix
N	Capillary tip concentration
B	Capillary sprout concentration
W	Oxygen concentration
M	Macrophage concentration
A	Chemoattractant concentration
F	Fibroblast concentration
P	Extracellular matrix concentration
ACL	Anterior cruciate ligament
H	Vibration frequency input

Introduction

When wounding occurs, the body immediately initiates a three-phase wound healing process. These three phases are: inflammation, proliferation, and remodeling [1]. Biological components that affect these phases of healing include: cells such as macrophages, fibroblasts, and endothelial cells, chemicals such as vascular endothelial growth factor (VEGF) and transforming growth factor beta (TGF- β), and finally, surrounding tissues such as the extracellular matrix (ECM) [2], which initiates biomechanical and biochemical cues for tissue morphogenesis [3]. The relationships between these components are very complex but the fundamental physiology is understood well enough to create mathematical representations [2].

A significant amount of progress has been made in mathematically modeling of the wound healing process [1, 4-6]. Various models have represented normal wound healing as well as delayed healing from ischemic conditions and diabetes [1, 7]. However, to date, there has only been one model that represents the healing process with a specific treatment modality [1]. The advantage of modeling and validating healing under treatment is to reveal the mechanisms by which the treatment is being effective. This could lead to more effective care via optimal treatment strategies.

This work is the first to develop a wound healing model with a mechanical treatment, specifically vibration therapy, and is referred to as the vibration enhanced wound healing (VEWH) model. Vibration literature has expanded rapidly over the past 20 years, and vibration therapy has been used for muscle recovery [8,9], increasing blood flow [10-16], and maintaining muscle activation levels [17]. However, there are relatively few studies analyzing vibration induced wound healing [18-21]. The VEWH model put forth in this work is an effort to represent and better understand how vibration promotes wound closure. Based on current data, the VEWH model can also be used to predict optimal duration and frequency of treatment, and complete time to wound closure.

Modeling Normal Wound Healing

Schugart et al. [1] developed a seven parameter, healthy wound healing model with an input of hyperbaric oxygen treatment. This model revealed the effect of tissue oxygen on the wound healing process and specifically angiogenesis. The seven variables of this model are capillary tips (n) and sprouts (b), oxygen (w), inflammatory cells or macrophages (m), chemoattractants (a), fibroblasts (f), and extracellular matrix (ρ). The seven, non-dimensionalized, partial differential equations are given below, and all parameter values are included in Table 1.

$$\partial n/\partial t = \nabla \cdot (D_n \nabla n - \rho n H(1-n) x_n \nabla a) + (a b \lambda_1 + a n \lambda_2) H(1-n) - (b \lambda_3 + n \lambda_4) n \quad (1)$$

$$\partial b/\partial t = \nabla \cdot (D_b \nabla b + A b D_n \nabla n - A b \rho n H(1-n) x_n \nabla a) + b (1-b) \lambda_5 G_b(w) \quad (2)$$

$$\partial w/\partial t = \nabla \cdot (D_w \nabla w) + w b \lambda_6 - (f \lambda_7 + m \lambda_8) w \quad (3)$$

$$\partial m/\partial t = \nabla \cdot (D_m \nabla m + m H(1-m) x_m \nabla w) - m \lambda_9 \quad (4)$$

$$\partial a/\partial t = \nabla \cdot (D_a \nabla a) + m \lambda_{10} G_a(w) - (n \lambda_{11} + b \lambda_{12} + \lambda_{13}) a \quad (5)$$

$$\partial f/\partial t = \nabla \cdot (D_f \nabla f - f H(1-f) x_f \nabla a) + f (1-f) \lambda_{14} G_f(w) - f \lambda_{15} \quad (6)$$

$$\partial \rho/\partial t = \nabla \cdot (D_\rho \nabla \rho + B \rho D_f \nabla f - B \rho f H(1-f) x_f \nabla a) + f (1-\rho) \lambda_{16} \quad (7)$$

Parameter/Function	Value	Physical Definition
D_n	1×10^{-3}	Tips diffusion coefficient
D_b	7×10^{-4}	Sprouts diffusion coefficient
D_w	0.5	Oxygen diffusion coefficient
D_m	0.05	Macrophage diffusion coefficient
D_a	1	Chemoattractant diffusion coefficient
D_f	1.7×10^{-4}	Fibroblast diffusion coefficient
D_ρ	1×10^{-5}	ECM diffusion coefficient
x_n	1	Tips chemotactic coefficient
x_m	0.1	Macrophage chemotactic coefficient
x_f	0.1	Fibroblast chemotactic coefficient
A	1	Capillary tip velocity coefficient
B	1	ECM velocity coefficient
λ_1	0.216	Growth of tips due to sprouts
λ_2	0.0216	Growth of tips due to tips
λ_3	0.0225	Death of tips due to sprouts
λ_4	0.225	Death of tips due to tips
λ_5	0.225	Growth of sprouts
λ_6	0.1388	Increase of oxygen due to sprouts
λ_7	0.277	Uptake of oxygen from fibroblasts
λ_8	4.16	Uptake of oxygen from macrophages
λ_9	0.045	Death rate of macrophages
λ_{10}	50	Increase of chemoattractant from macrophages
λ_{11}	9	Uptake of chemoattractant by tips
λ_{12}	90	Uptake of chemoattractant by sprouts
λ_{13}	0.9	Uptake of chemoattractant
λ_{14}	0.25	Growth of fibroblasts
λ_{15}	5.2×10^{-3}	Death of fibroblasts
λ_{16}	0.25	Growth of ECM from fibroblasts
∇	NA	Spatial gradient
$H(x)$	0 for $x < 0$ 1 for $x \geq 0$	Heaviside step function
$G_b(w)$	0 for $0 \leq w < 0.5$ $2w-1$ for $w \geq 0.5$	Tissue oxygen tension function
$G_a(w)$	$3w$ for $0 \leq w < 0.5$ $2-w$ for $0.5 \leq w < 1$ w for $w \geq 1$	Tissue oxygen tension function
$G_f(w)$	$G_b(w)$	Tissue oxygen tension function
$G(w)$	$G > 0$	Hyperbaric oxygen intervention

Table 1: Parameter values and their physical meaning for Schugart Model

Figure 1 shows the body’s complex, non-linear response to healing. When a wound occurs, inflammatory cells (ie. Macrophages) immediately infiltrate the wound to remove bacteria and dead tissue. While removing dead tissue, macrophages are guided by mechanical stimuli and begin depositing chemoattractants such as VEGF and TGF-β (Fig. 1a). These chemoattractants recruit capillary tips and sprouts to grow into the wound, as well as fibroblasts (Fig. 1b). The capillary tips and sprouts are guided by chemoattractant and ECM (Fig. 1c) while providing much needed oxygen, via blood flow, to the macrophages and fibroblast cell populations so they can continue to perform their respective functions (Fig. 1c). The fibroblasts are guided by chemoattractant and mechanical stimuli to deposit ECM, to quickly close the wound and reduce the likelihood of infection (Fig. 1b). This ECM is the precursor to scar tissue and it also helps direct the capillary growth in the wound.

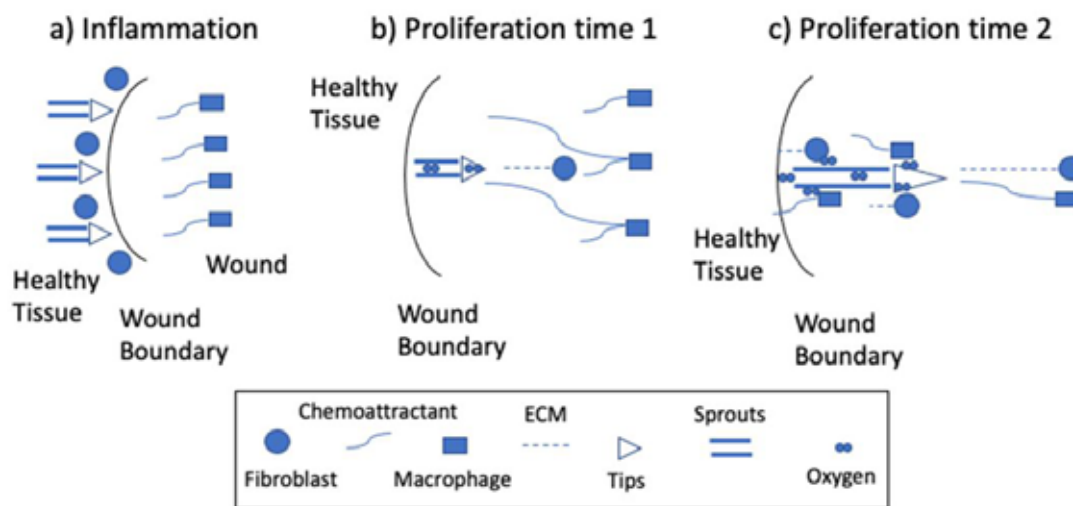


Figure 1: Normal wound healing process based on the proposed model by Schugart et al

Parameter values for the Schugart model were selected from applicable experimental data. In the case where experimental data was non-existent, Schugart et al. chose values “such that healing of the mouse wound should be completed in ~10 days” [1]. Furthermore, they defined healing as re-epithelialization of the wound being completed. The parameters with values selected to meet the 10-day criterion are: λ_{10} , λ_{14} , and λ_{16} . These parameters represent the growth rate of chemoattractant proportional to macrophages, the growth rate of fibroblasts proportional to oxygen, and the growth of ECM proportional to fibroblasts, respectively.

The VEWH Model

The Schugart model was adjusted to represent un-aided, healthy, wound healing in the VEWH model. This was done by replacing the hyperbaric oxygen input ($G(w)$) with the oxygen concentration (w), increasing λ_{10} from 50 to 70, decreasing λ_{14} from 0.25 to 0.1, and increasing λ_{16} from 0.25 to 0.75, so the ECM concentration of un-aided healing represents wound closure of mice wounds reported in the experimental data [19, 22]. The vibration terms that are included in the VEWH are derived from published experimental data as detailed in the following sections.

Vibration Effected Parameters

There are five vibration effected parameters in the VEWH model. These are capillary tips and sprouts, macrophages and chemoattractants, and fibroblasts. Figure 2 shows how vibration impacts these healing components. Vibration increases blood flow in capillaries which results in greater capillary tip and sprout growth [18-20]. Macrophage and fibroblast cells convert mechanical signals into cellular proliferation and activation. This leads to greater growth of those cells as well as an increase in both chemoattractant production by macrophages and ECM production by fibroblasts [23-25].

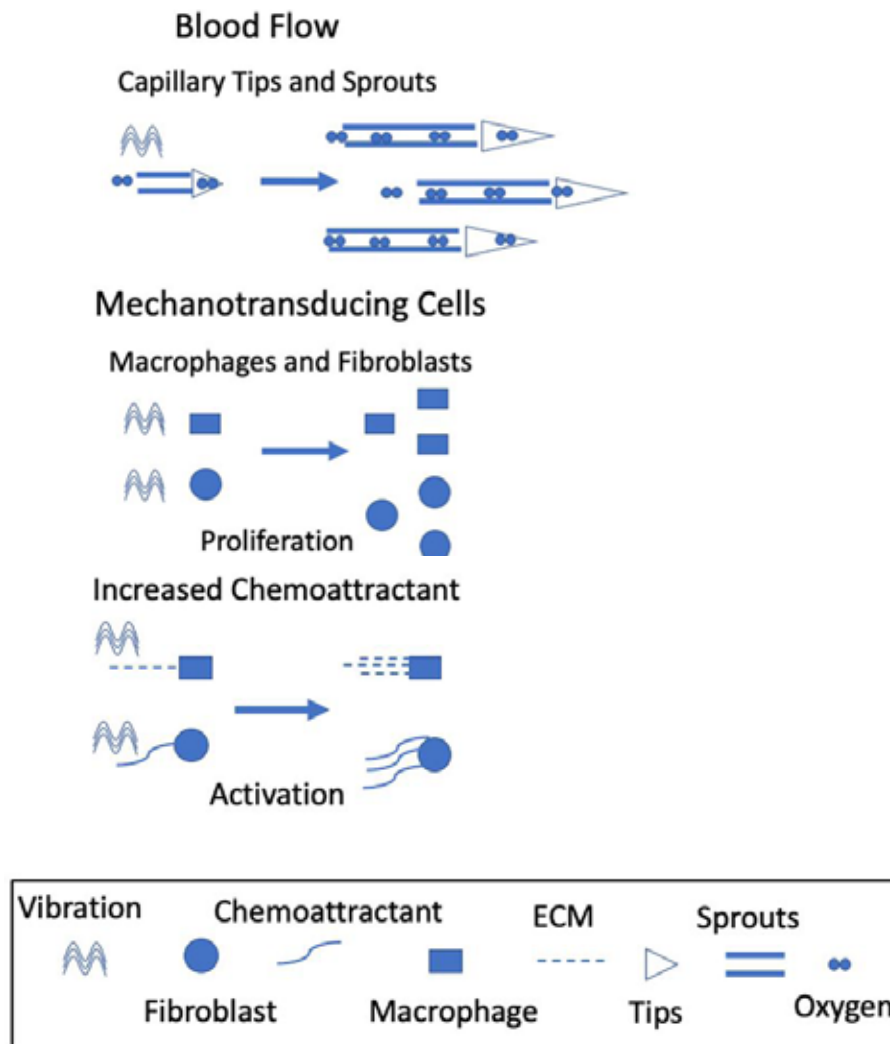


Figure 2: Vibration impact on capillary tips and sprouts, macrophages, fibroblasts, and chemoattractant

Vibration Impacts Capillaries Through Blood Flow

Efforts have been made to measure the effect of vibration on angiogenesis [18-20], yet the mechanism through which this occurs is still unclear. It has been shown that whole body vibration increases blood flow [12-16] and there appears to be a relationship between frequency and the blood velocity increase [16]. It is our hypothesis that vibration increases wound angiogenesis by increasing blood flow to the wound site. We have modeled this increase by including Eq. (15) in Eqs. (8, 9) to represent the percent increase in blood velocity (V_{cap}) times the capillary tip and sprout concentrations. This assumes a linear relationship between blood velocity and capillary growth, as well as assuming that capillary tips and sprouts are equally impacted by increased blood velocity.

Equation (15) was derived from experimental data on vibration and blood flow [12-15]. These studies measured the percent increase in blood velocity after whole body vibration treatment. The location of blood velocity measurement was either the popliteal or the femoral artery, leading to consistency in the reported results. Equation (15) fits the data with a correlation coefficient $R^2 = 0.999$ and this equation shows that blood flow peaks with a vibration frequency of 30 Hz. This is consistent with the consensus that blood flow is excited more with lower frequency vibration compared to higher frequencies [11].

Vibration Impacts Macrophages and Fibroblasts Through Mechano transduction

Macrophages and fibroblasts are mechano transducing cells that alter activation and proliferation due to mechanical stimuli. The way mechanical signals are transmitted to these cells is via actin filaments that connect to the ECM [25, 26]. This means that as

the ECM grows, more adhesion sites are generated, and macrophage and fibroblast cells can sense more vibration. Therefore, Eqs. (11, 13) have an additional term $V_{mac} * m * (1 + \rho)$ and $V_{fib} * f * (1 + \rho)$ respectively. V_{mac} and V_{fib} represent the increase in macrophage or fibroblast concentration due to vibration as a function of frequency, and $(1 + \rho)$ represents the percent increase of ECM from the wounded state [23, 24]. The increase in macrophage concentration also has a significant impact on chemoattractant production [23]. This is represented in Eq. (12) as $V_{att} * m * \lambda_{10} * G_a(w)$ to model the increase of chemoattractant concentration being proportional to the increase of macrophage density.

Equation (16) was derived from data reported by Pongkitwitoon et al. [23] where collected macrophage cells were vibrated in vitro at different frequencies to measure the frequency impact on cell proliferation [23]. Equation (16) shows that the number of macrophage cells parabolically increases with frequency and the correlation coefficient for this data fit is $R^2 = 1.00$.

Interestingly, Pongkitwitoon et al. also measured how vibration influenced the production of VEGF and TGF- β which are represented in the VEW model as a single chemoattractant term. They reported that VEGF significantly increased with vibration frequency but TGF- β was impacted much less [23]. To model the VEGF, we derived the effect of frequency on chemoattractant from the VEGF data reported by Pongkitwitoon et al. This resulted in Eq. (17) with a correlation coefficient $R^2 = 1.00$.

Finally, Eq. (18) was derived from Jiang et al. and their experimental work on the anterior cruciate ligament (ACL) fibroblasts in vitro. As represented in Eq. (18) the number of fibroblast cells increases with an increase in vibration frequency until 12 Hz after which it decreases with increasing frequency [24]. One concern from this study is that it may not be an accurate representation of a wound scenario. The initial number of fibroblasts was 5.0×10^4 and the control case saw that number triple to 15.0×10^4 cells after 4 days [24]. Furthermore, when the control data was included at 0 Hz vibration the VEW model did not converge to the adjusted Schugart model of non-vibration enhanced, normal healing. Therefore, the VEW model neglects the control case presented by Jiang et al. [24] and Eq. (18) has an initial value of -0.7143. After incorporating this new control value, the correlation coefficient for the remaining data fit is $R^2 = 1.00$. The Jiang et al. study is the only one that examined vibration impact on fibroblast cells. There may be a difference in the response of cutaneous fibroblasts compared to ACL fibroblasts, but the VEW model assumes a similar response between the cells in either tissue.

Indirect Vibration Terms

Vibration has not been shown to directly affect oxygen concentration nor extracellular matrix. Therefore, Eqs. (10, 14) remain equivalent to Eqs. (3, 7). However, Eq. (10) is coupled with Eq. (9) as the oxygen concentration increases proportionally to the capillary sprout concentration. Similarly, Eq. (14) is coupled with Eq. (13) due to the proportional increase of ECM to fibroblast concentration. This reveals that vibration does not directly impact oxygen nor ECM concentrations, but they are affected indirectly by capillary sprouts and fibroblasts respectively.

VEW Model Equations

Equations 1, 2, and 4-6 were given vibration terms that are frequency (h) dependent based on the respective evidence for capillary tips and sprouts, macrophages, chemoattractant, and fibroblasts. These adjusted equations are given below as Eqs. (8-14), and the functions for the vibration parameters are given as Eqs. (15-18) with vibration parameter values in Table 2.

$$\partial n / \partial t = \nabla \cdot (D_n \nabla n - \rho n H(1-n) x_n \nabla a) + (a b \lambda_1 + a n \lambda_2) H(1-n) - (b \lambda_3 + n \lambda_4) n + n V_{cap} \tag{8}$$

$$\partial b / \partial t = \nabla \cdot (D_b \nabla b + A b D_n \nabla n - A b \rho n H(1-n) x_n \nabla a) + b (1-b) \lambda_5 G_b(w) + b V_{cap} \tag{9}$$

$$\partial w / \partial t = \nabla \cdot (D_w \nabla w) + w b \lambda_6 - (f \lambda_7 + m \lambda_8) w \tag{10}$$

$$\partial m/\partial t = \nabla \cdot (D_m \nabla m + m H(1-m) x_m \nabla w) - m \lambda_9 + m(1+\rho) V_{\text{mac}} \quad (11)$$

$$\partial a/\partial t = \nabla \cdot (D_a \nabla a) + m \lambda_{10} G_a(w) - (n \lambda_{11} + b \lambda_{12} + \lambda_{13}) a + m V_{\text{att}} \lambda_{10} G_a(w) \quad (12)$$

$$\partial f/\partial t = \nabla \cdot (D_f \nabla f - f H(1-f) x_f \nabla a) + f(1-f) \lambda_{14} G_f(w) - f \lambda_{15} + f(1+\rho) V_{\text{fib}} \quad (13)$$

$$\partial \rho/\partial t = \nabla \cdot (D_\rho \nabla \rho + B \rho D_f \nabla f - B \rho f H(1-f) x_f \nabla a) + f(1-\rho) \lambda_{16} \quad (14)$$

$$V_{\text{cap}} = v_8 h^3 + v_9 h^2 + v_3 h + v_4 \quad (16)$$

$$V_{\text{mac}} = v_5 h^2 + v_6 h \quad (17)$$

$$V_{\text{att}} = v_7 h^2 + v_8 h \quad (18)$$

$$V_{\text{fib}} = v_9 + v_{10} A h^4 + v_{11} h^3 + v_{12} h^2 + v_{13} h \quad (19)$$

Parameter	Value
v_1	-5.449×10^{-7}
v_1	1.559×10^{-5}
v_2	-1.897×10^{-3}
v_3	0.07201
v_4	-2.046×10^{-14}
v_5	7.618×10^{-5}
v_6	6.383×10^{-3}
v_7	-1.286×10^{-4}
v_8	0.02886
v_9	-0.7143
v_{10}	8.972×10^{-7}
v_{11}	-5.140×10^{-5}
v_{12}	6.037×10^{-4}
v_{13}	-3.984×10^{-3}

Table 2: Vibration parameter values for VEWH model

Results

This section presents the results of the VEWH model and compares them to a non-vibration based (normal) wound healing model, and both vibration enhanced, and non-vibration enhanced (normal) experimental wound healing data. The oxygen concentration adjusted Schugart et al. [1] model is used as the non-vibration based model. The only published vibration enhanced healing data for healthy mice are presented by Yu et al. [19]. Wounds in this study initially expanded after one day, so wound closure was calculated from the largest reported size and set as day 0 [19].

The VEWH model prediction, the oxygen adjusted Schugart model, and the Yu et al. experimental normal and vibration enhanced wound healing data are shown in Fig. 3. The vibration treatment for the data shown in Fig. 3 consisted of 20 minutes of vibration at 35 Hz for 5 days per week, which was replicated in the VEWH model simulations.

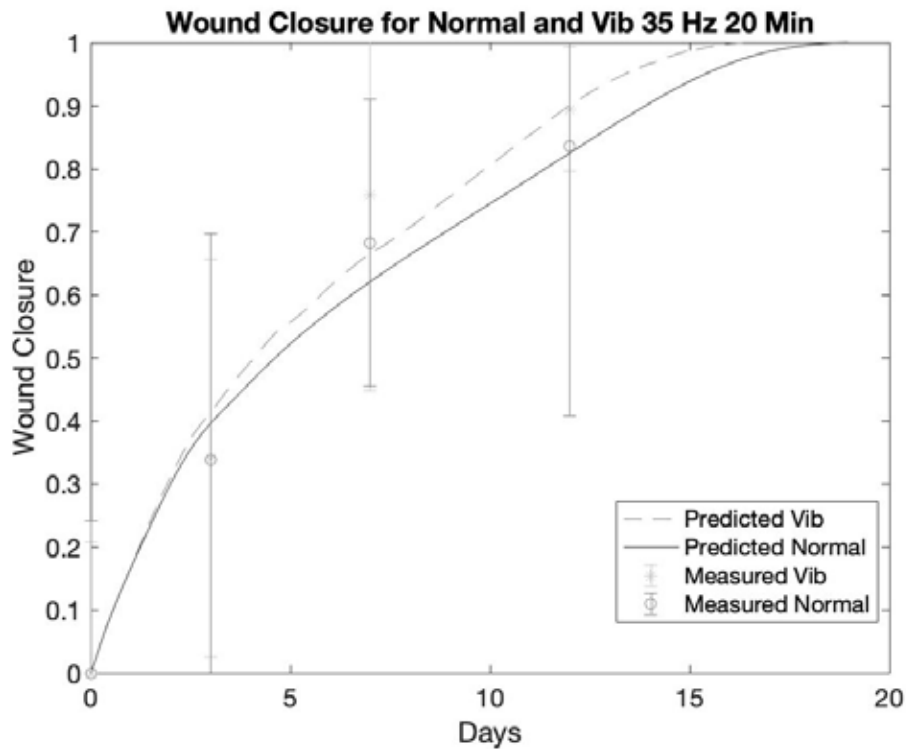


Figure 3: Predicted and measured wound closure rates for normal and vibration healing

The VEWH model prediction starts to diverge from the non-vibration based Schugart model at about day 2.5. There is an increased healing rate in the vibration enhanced results between about days 3-5. Then the healing rate is relatively constant between the VEWH and normal models. The VEWH model predicts complete wound closure 2.5 days before the normal model. The relatively large standard deviation bars indicate the high level of uncertainty in the experimental data. Table 3 shows the standard deviations of the experimental data as well as the percent error of the non-vibration enhanced (normal) and the VEWH simulations compared with the average wound closure reported by Yu et al [19]. As noted, the experimentally measured data have a high degree of uncertainty, which leads to greater percent error in the model simulations. The VEWH simulation with vibration treatment at 35 Hz for 20 min/day, predicts that wounds of healthy mice close 13.0% faster compared to normal healing. It is noted that there is significantly less error in the model and experimental data as the wound closes.

Day	Experimental Data % Closed (\pm std)		Model Prediction % Closed (% error)	
	Normal	VEWH	Normal	VEWH
3	34 (36)	34 (\pm 31)	39 (-17)	41 (-21)
7	68 (\pm 23)	76 (\pm 31)	62 (9)	66 (12)
12	84(43)	89 (\pm 10)	83 (1)	89 (-1)

Table 3: Experimental data and model prediction for normal and vibration healing

If we adjust the vibration treatment by varying the frequency, we can see that lower frequencies (<25 Hz) have the greatest impact on closure rate as shown in Fig. 4. From this plot we also see that normal healing takes 18.9 days to heal, while vibration treatment at 15 Hz closes the wound 16.0% faster (15.9 days) and vibration treatment at 5 Hz closes the wound 10.0% faster (17.0 days). It is also evident that frequencies greater than 45 Hz become destructive, as the closure rate at 45 Hz nearly matches normal wound healing.

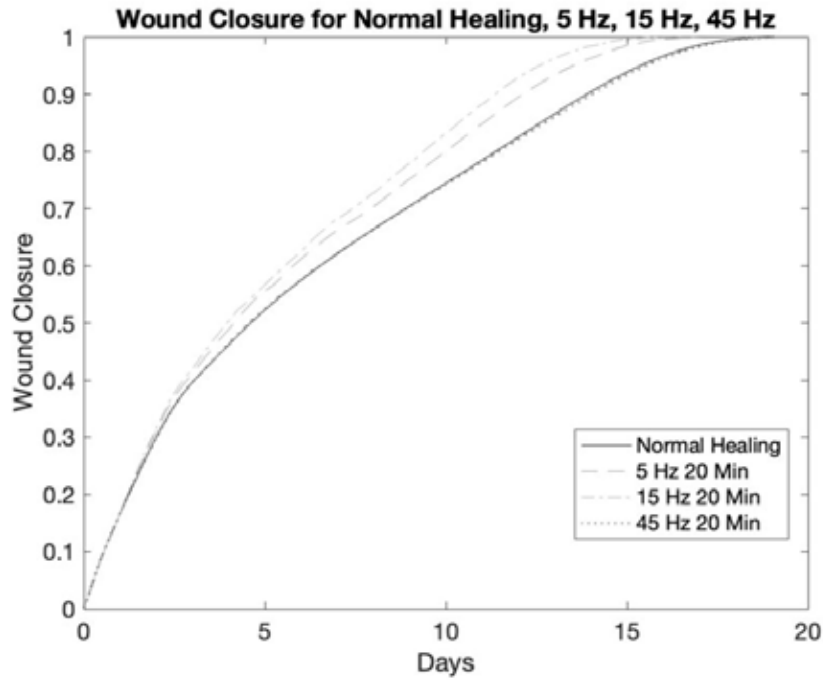


Figure 4: Effect of varying vibration frequency on wound closure rate

Figure 5 shows the effect of varying the amount of time of vibration treatment. Here we see that increasing treatment time increases healing rate more than a change in vibration frequency.

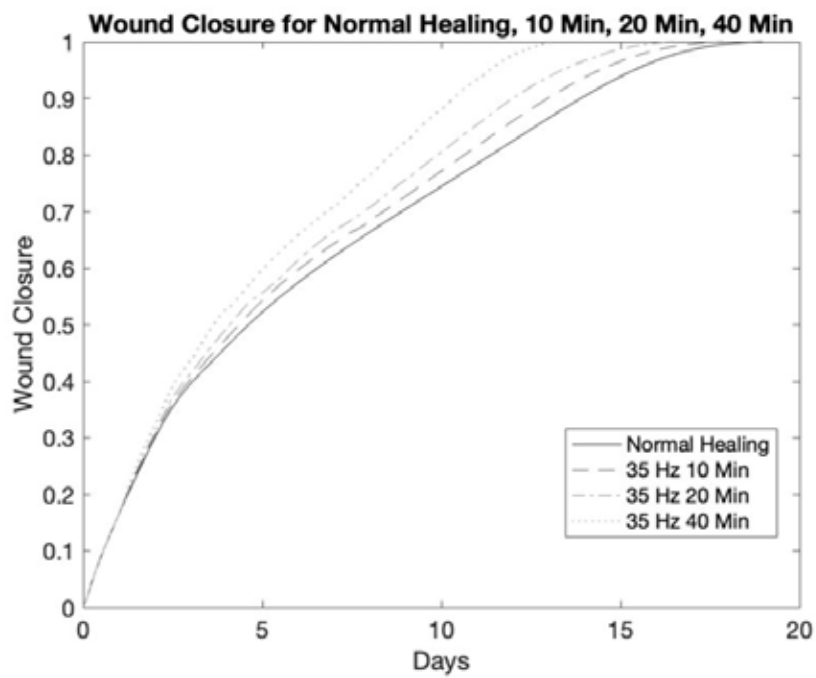


Figure 5: Effect of varying treatment time on wound closure rate

Table 4 shows the number of days it takes for a wound to close and the percent decrease in closure time, for several frequencies. From this table we see that 5 Hz and 25 Hz have the same closure rate. This suggests that the optimal treatment frequency is between 5 Hz and 25 Hz. Table 5 shows the closure predictions for varying treatment times. The frequency 35 Hz is used for varying treatment times because that was the frequency used by Yu et al. Similarly, for varying frequencies, 20 minutes is used as the treatment time [19].

Frequency (Hz)	Time (min)	Days to Closure	% Decrease of time to Closure
0	0	18.9	NA
5	20	17.0	10.0
10	20	15.9	16.0
15	20	15.9	16.0
25	20	17.0	10.0
35	20	16.4	13.0
45	20	19.0	-0.7

Table 4: Days to closure and percent decrease of closure time compared to baseline for various frequencies

Frequency (Hz)	Time (min)	Days to Closure	% Decrease of time to Closure
0	0	18.9	NA
35	10	17.8	5.7
35	20	16.4	13.0
35	30	15.7	17.0
35	40	13.1	30.7

Table 5: Days to closure and percent decrease of closure time compared to baseline for various treatment times

Discussion

One of the goals of the VEWH model was to investigate the mechanism through which vibration accelerates wound closure. This was done by systematically removing vibration terms for capillary tips and sprouts, fibroblasts, macrophages, and/or chemoattractant. Simulations were run with a single vibration parameter included and then successively adding terms back in. Initially, Eqs. (16-18) were removed to determine wound closure’s dependence on blood flow. This showed a very small increase in healing. This was somewhat surprising that healing isn’t more dependent on blood flow which was our hypothesis. Next, Eq. (15) was removed, and Eq. (16) was added back to the model to find the dependence of healing on macrophages. This revealed that macrophages have a small negative effect on healing. This may be due to macrophage’s consumption of oxygen which reduces the amount of oxygen available to fibroblasts. Thus, hindering fibroblasts’ ability to deposit ECM. Then, Eq. (16) was removed and Eq. (17) was added back to the model, to find the dependence on chemoattractant. This simulation showed no impact on healing. This may be because chemoattractants recruit both macrophages and fibroblasts resulting in a neutral impact on healing. Finally, Eq. (17) was removed and Eq. (18) was added to the model. This revealed that fibroblasts play the largest role in wound closure, likely because these cells deposit the proteins that make up the ECM. From this, we can conclude that the effect of vibration on fibroblasts is the primary mechanism through which vibration accelerates wound closure.

The experimental data for healthy mice, clearly show an increase in wound closure rate due to vibration therapy [19]. There is even greater evidence for vibration accelerated wound closure in diabetic mice [18-21]. Diabetes is known to delay normal wound healing and was not considered in creating this VEWH model. As such, one of the limitations of the VEWH model is the lack of validation data for vibration accelerated healthy wound healing and the uncertainty associated with the published data. Despite this need for more experimental validation, the VEWH model is a first step in modeling mechanically aided cutaneous wound healing in the form of vibration.

Another limitation of the VEWH model is the frequency range explored by the experimental data. Only three frequencies (35 Hz, 45 Hz, and 90 Hz) were used in the four studies that investigated vibration therapy on wound healing [18-21]. Furthermore, studies that found a relationship between vibration and healing components typically used only one or two frequencies, usually between 10 Hz and 50 Hz [12-15, 23, 24]. This means that the VEWH model should only be considered for frequencies from 10 Hz to 55 Hz, any extrapolation beyond this range will have very low confidence. It has also been found that the relationship between blood flow and vibration is dependent on the type of vibration, not just the frequency. Studies show that oscillating platforms result in low frequencies impacting blood velocity while vertical vibration platforms are more inconclusive [11, 16].

Despite these limitations, the VEWH model can be used to draw significant conclusions regarding vibration and wound healing. We can predict that frequencies between 5 Hz and 25 Hz have the largest benefit to wound closure rate in healthy subjects. In addition, we hypothesize that this very complex system is primarily impacted through the fibroblast cell population. With more targeted experimentation, the VEWH model will serve as a steppingstone to more accurate predictive models and optimization for the mechanical treatment of wound healing.

Conclusion

This first model of mechanically stimulated wound healing is supported by existing experimental data. Despite the need for further experimental validation, it does show that the rate of wound healing can be increased with vibration treatment (ie. 15 Hz for 40 minutes). This has important implications for populations that experience chronic wounds or those who suffer from delayed wound healing. The VEWH model shows that vibration treatments with 15 Hz for 40 minutes/day can lead to accelerated healing which may be a safer or more cost-effective treatment than pharmaceutical or surgical measures. Finally, the VEWH model identifies the ability of the fibroblasts to transduce mechanical vibrations into greater ECM production as the primary mechanism by which vibration increases wound closure rates.

References

1. Richard CS, Friedman A, Zhao R, Chandan KS (2008) "Wound Angiogenesis as a Function of Tissue Oxygen Tension: A Mathematical Model." *Proceedings of the National Academy of Sciences - PNAS* 105: 2628-33.
2. Stephanie NJ, Sanders JR (2015) "Mathematical Models of Wound Healing and Closure: A Comprehensive Review." *Medical & Biological Engineering & Computing* 54:1297-16.
3. Frantz C, Stewart KM, Weaver VM (2010) The extracellular matrix at a glance. *J Cell Sci.* 123:4195-4200.
4. Koppenol DC, Vermolen FJ, Niessen FB, van Zuijlen PPM, Vuk K (2017) "A Mathematical Model for the Simulation of the Formation and the Subsequent Regression of Hypertrophic Scar Tissue After Dermal Wounding". *Biomechanics and Modeling in Mechanobiology* 16:15-32.
5. Jonathan AS, Dallon JC (2002) "Theoretical Models of Wound Healing: Past Successes and Future Challenges." *Comptes Rendus. Biologies*, 325:557-64.
6. Cumming BD, McElwain DLS, Upton Z (2010) "A Mathematical Model of Wound Healing and Subsequent Scarring." *Journal of the Royal Society Interface* 7:19-34.
7. Chuan X, Friedman A, Sen CK (2009) "A Mathematical Model of Ischemic Cutaneous Wounds." *Proceedings of the National Academy of Sciences - PNAS* 106:16782-87.
8. Jones GC, Blotter JD, Smallwood CD, Eggett DL, Cochrane DJ, Feland JB (2021) "Effect of Resonant Frequency Vibration on Delayed Onset Muscle Soreness and Resulting Stiffness as Measured by Shear-Wave Elastography." *International Journal of Environmental Research and Public Health* 18:10.
9. Pournot H, Tindel J, Testa R, Mathevon L, Lapole T(2016) "The Acute Effect of Local Vibration as a Recovery Modality from Exercise-Induced Increased Muscle Stiffness." *Journal of Sports Science & Medicine* 15:142-47.
10. Mahbub MH, Hiroshige K, Yamaguchi N, Hase R, Harada N, Tanabe T (2019) "A Systematic Review of Studies Investigating the Effects of Controlled Whole-body Vibration Intervention on Peripheral Circulation." *Clinical Physiology and Functional Imaging* 39:363-77.
11. Games KE, Sefton JM, Wilson AE (2015) Whole-body vibration and blood flow and muscle oxygenation: a meta-analysis. *J Athl Train.* 50:542-49.
12. Sanudo, B, Rosa RA, Cruz BDP, Cruz JDP, Galiano D, Figueroa A (2013) "Whole Body Vibration Training Improves Leg Blood Flow and Adiposity in Patients with Type 2 Diabetes Mellitus." *European Journal of Applied Physiology* 113:2245-52.
13. Hazell TJ, Thomas GW, Deguire JR, Lemon PW (2008) "Vertical Whole-Body Vibration does Not Increase Cardiovascular Stress to Static Semi-Squat Exercise." *European Journal of Applied Physiology* 104:903-08.
14. Menendez HJ, Hernandez M, Ferrero C, Figueroa A, Herrero AJ, Marin PJ (2015) "Influence of Isolated Or Simultaneous Application of Electromyostimulation and Vibration on Leg Blood Flow." *European Journal of Applied Physiology* 115:1747-55.

15. Schindl K, Grampp KS, Henk C, Resch H, Preisinger E, Moser VF, Imhof H (2001) "Whole-Body Vibration Exercise Leads to Alterations in Muscle Blood Volume." *Clinical Physiology (Oxford, England)* 21:377-82.
16. Lythgo N, Eser P, de Groot P, Galea M (2009) Whole-body vibration dosage alters leg blood flow. *Clin Physiol Funct Imaging*. 29:53-9.
17. Dickerson C, Gabler G, Hopper K, Kirk D, McGregor CJ (2012) "Immediate Effects of Localized Vibration on Hamstring and Quadriceps Muscle Performance." *International Journal of Sports Physical Therapy* 7:381-87.
18. Haus W, Eileen M, Judex S, Ennis WJ, Koh TJ (2014) "Low-Intensity Vibration Improves Angiogenesis and Wound Healing in Diabetic Mice." *PloS One* 9:e91355.
19. Yu, Oi-Ling C, Leung KS, Jiang JL, Wang TBY, Chow SKH, Cheung WH (2017) "Low-Magnitude High-Frequency Vibration Accelerated the Foot Wound Healing of N5-Streptozotocin-Induced Diabetic Rats by Enhancing Glucose Transporter 4 and Blood Microcirculation." *Scientific Reports* 7:11631-12.
20. Roberts RE, Bilgen O, Kineman RD, Koh TJ (2021) "Parameter-Dependency of Low-Intensity Vibration for Wound Healing in Diabetic Mice." *Frontiers in Bioengineering and Biotechnology*, 9: 654920.
21. Wano N, Sanganrungsirikul S, Keelawat S, Somboonwong J (2021) "The Effects of Whole-Body Vibration on Wound Healing in a Mouse Pressure Ulcer Model." *Heliyon* 7:e06893.
22. Ishida Y, Kuninaka Y, Nosaka M, Furuta M, Kimura A, Taruya A, Yamamoto H et al. (2019) "CCL2-Mediated Reversal of Impaired Skin Wound Healing in Diabetic Mice by Normalization of Neovascularization and Collagen Accumulation." *The Journal of Investigative Dermatology* 13:2517-27.e5.
23. Pongkitwitoon, S., E. M. Weinheimer-Haus, T. J. Koh, and S. Judex. 2016. "Low-Intensity Vibrations Accelerate Proliferation and Alter Macrophage Phenotype in Vitro." *Journal of Biomechanics* 49:793-96.
24. Jiang YY, Park JK, Yoon HH, Choi H, Kim CW, Seo YK (2015) "Enhancing Proliferation and ECM Expression of Human ACL Fibroblasts by Sonic Vibration." *Preparative Biochemistry & Biotechnology* 45: 476-90.
25. Kim D, Kwon S (2020) "Vibrational Stress Affects Extracellular Signal-Regulated Kinases Activation and Cytoskeleton Structure in Human Keratinocytes." *PloS One* 15:e0231174.
26. Ohashi K, Fujiwara S, Mizuno K (2017) "Roles of the Cytoskeleton, Cell Adhesion and Rho Signalling in Mechanosensing and Mechanotransduction." *Journal of Biochemistry* 161:245-54.

Submit your next manuscript to Annex Publishers and benefit from:

- ▶ Easy online submission process
- ▶ Rapid peer review process
- ▶ Online article availability soon after acceptance for Publication
- ▶ Open access: articles available free online
- ▶ More accessibility of the articles to the readers/researchers within the field
- ▶ Better discount on subsequent article submission

Submit your manuscript at
<http://www.annexpublishers.com/paper-submission.php>